Earthquake rupture inversions:

the (ugly) past
the (not-quite-as-ugly) present
the (hopefully bright) future

A Primer

P. Martin Mai
King Abdullah University of Science & Technology
martin.mai@kaust.edu.sa

Know where you are ...

The 2008 May 29 earthquake doublet in SW Iceland

J. Decriem,[1] T. Árnadóttir,[1] A. Hooper,[2] H. Geirsson,[3] F. Sigmundsson,[1] M. Keiding,[1]
B. G. Ófeigsson,[1] S. Hreinsdóttir,[4] P. Einarsson,[1] P. LaFemina[5] and R. A. Bennett[4]

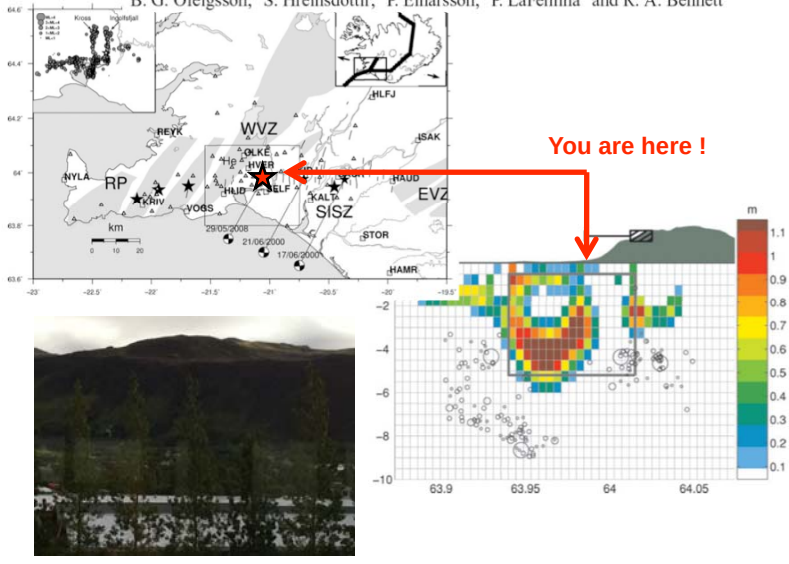

Overview

Goals for this introduction to earthquake sources

- Establish a general understanding of the kinematics of earthquake ruptures
- Introduce a few mathematical tools to describe earthquake ruptures and seismic wave generation
- Describe briefly how seismic data are used to estimate certain earthquake source properties from seismic waves

Earthquake source inversions are essential

- **to develop methods & models for near-field ground-motion simulation (for seismic hazard purposes)**
- **to study earthquake mechanics**
- **to build an understanding of earthquake dynamics**

3

Overview

Graphical illustration of a kinematic rupture model

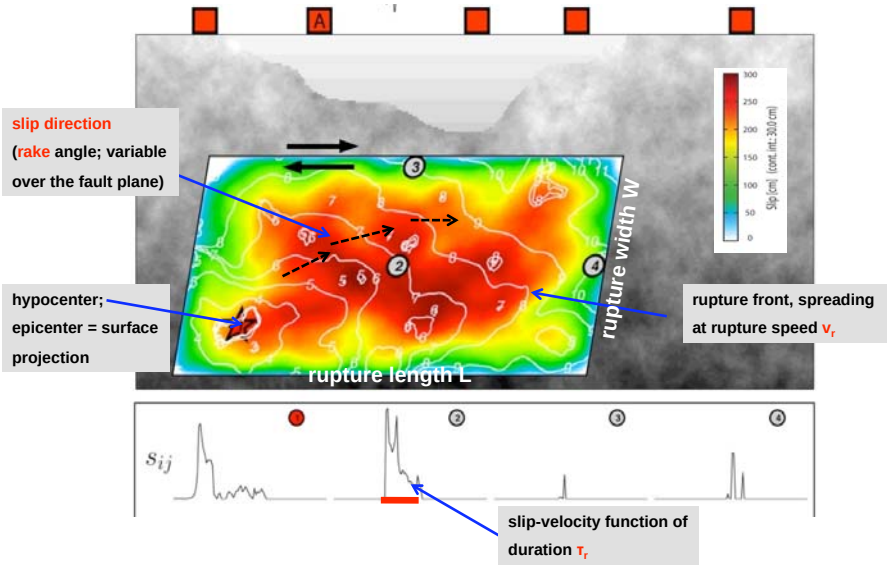

4

Definitions for some source parameters

- **rupture velocity:** v_r – the velocity with which the rupture front propagates over the entire fault plane (i.e. a macroscopic measure); generally 70-90% of shear-wave velocity (2 - 3 km/s)
- **slip velocity:** $\dot{\mathbf{u}}$ – the velocity with which each point on the fault moves (highly variable, generally 10-100 cm/s)
- **rupture duration:** T_r – time it takes for the earthquake to rupture the entire fault plane, i.e. from rupture nucleation until the last point on the fault stops slipping; related to rupture velocity; depends on earthquake size
- **slip duration:** τ_r – length of time that each point on the fault slips; highly variable on the fault plane; also called **rise time**; strongly influences ground-motions; scales with displacement
- **slip-velocity function (SVF)** $\dot{\mathbf{u}}(t)$ – functional form of slip-velocity with time which comprises some measure of rise time; its details have a strong influence on ground motions; classical SVF are boxcar or triangular functions, but don't consider the dynamics of earthquake rupture (crack models)
- **stress drop:** $\Delta\sigma$ – in the static sense, a simple measure of strain release (~ D/L, i.e. ratio of mean-slip D over some length scale L) used to denote radiation strength; from dynamic rupture modeling, stress drop is found to be heterogeneous on the fault

5

Overview
QUEST, July 12-17, 2011

Kinematic Earthquake Rupture Models

- Characterize the time-dependent displacement trajectory of points on the rupture plane **without** considering the forces/stresses that cause the motions. The rupture process is entirely specified by the spatio-temporal distribution of source parameters (slip, slip-velocity function, slip duration, rupture speed).
- Kinematic source models are obtained by seismic waveform modeling, i.e. by inverting near-field (strong-motion), regional-distance, and/or far-field (teleseismic) seismograms.
- For seismic-hazard studies, kinematic models are often "simply" simulated.

Dynamic Earthquake Rupture Models

- Characterize earthquake rupture based on the material properties around the source volume, and the initial & boundary conditions for the forces/stresses acting on the fault plane. The slip-velocity function at each point on the fault is obtained by solving the elasto-dynamic equations of motion under the assumption of some constitutive law.
- Dynamic rupture models are obtained from existing kinematic models by an inversion/modeling approach (rarely from waveforms directly), or for assumed initial conditions and stress distributions.

6

Seismic waves

- Generally, **seismic sources** produce seismic waves (body waves, surface waves, and perhaps measurable free oscillations of the Earth).
- The relative excitation of body (P- and S-) waves and surface waves, and their amplitude and frequency, depends strongly on the source type, the force-time history ("earthquake rupture process"), and Earth structure.
- Seismic recordings are also affected by source-site geometry, the very localized geology at the recording site ("site effects") and the recording device ("instrument response")

Seismic waves

- **Teleseismic recording** at distance of ~110°, showing prominent surface waves as well as several body-wave phases

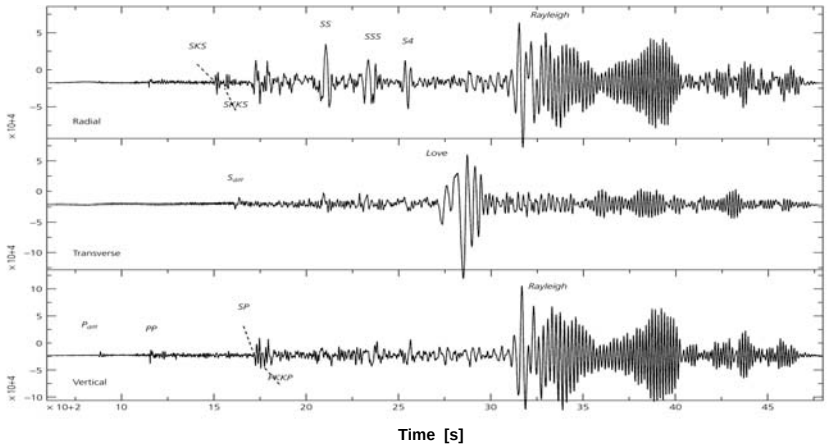

Seismic waves

- **Regional-distance recording** (m_b 6.3 earthquake) at distance of 6°

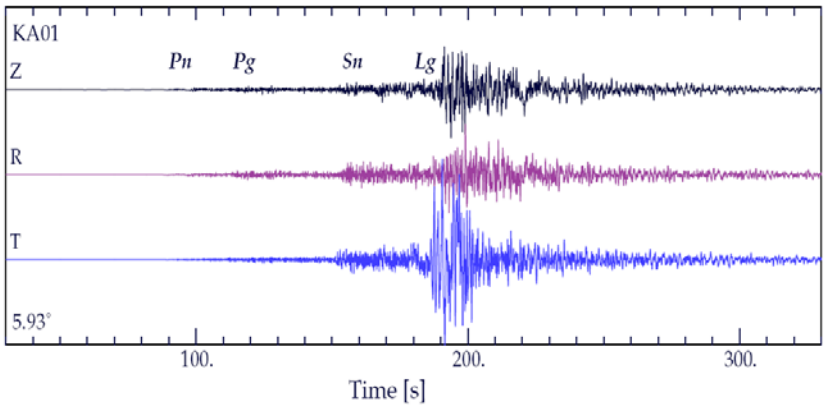

From B.L.N. Kennet (http://rses.anu.edu.au/~brian/ ; The Seismic Wavefield, I, II)

9

Seismic waves

- **Near-field recording** of the 1995 Kobe (M_w 6.9) earthquake (R = 18.5 km)

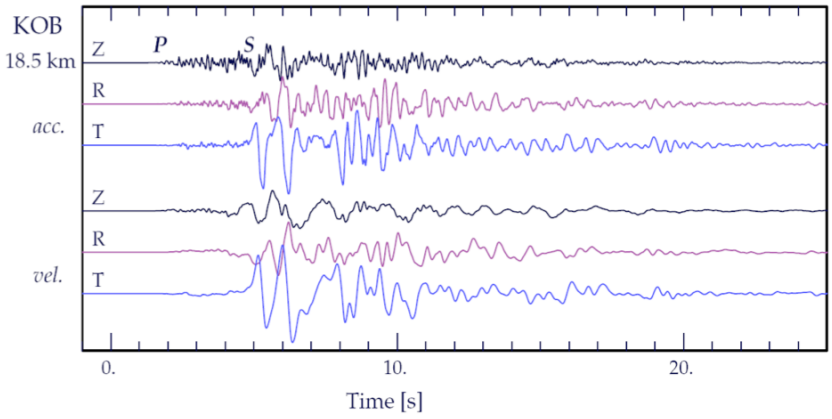

From B.L.N. Kennet (http://rses.anu.edu.au/~brian/ ; The Seismic Wavefield, I, II)

10

Motivation

Variability of near-field ground-motions

- **Example:** Ground-Velocities for the 2004 M_w 6 Parkfield earthquake

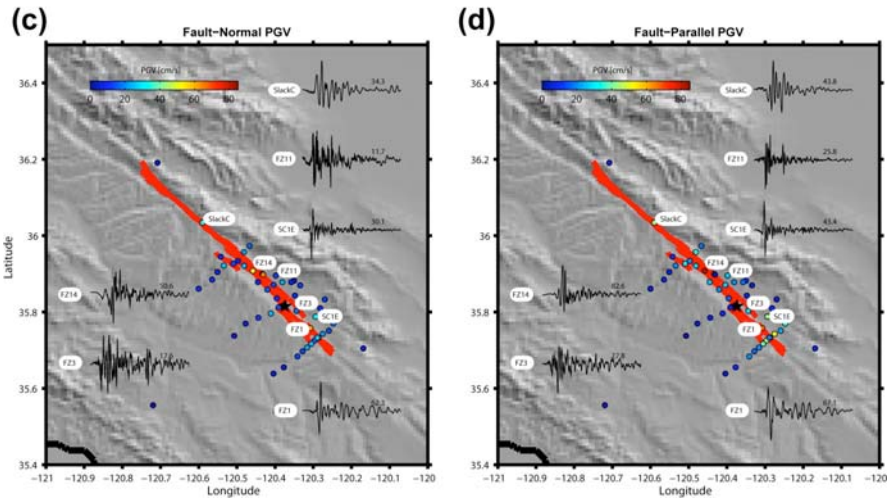

Mathematical tools

We need a quantitative description of the physical processes affecting ground-motion

- To be able to analyze ground-motion recordings (seismograms) and to investigate (and potentially separate) the different physical processes affecting the seismic recordings, we need a mathematical description for the ground-shaking induced by some (seismic) source and observed by a recording device.
- To first order, we can assume that this process is appropriately modeled by a linear operation: the excitation, propagation, and observation of “some signal” is described by **linear filter theory**.

Mathematical tools

Ground-motion computation

$$u_k(t) = s(t) * g_k(t) * i_k(t)$$

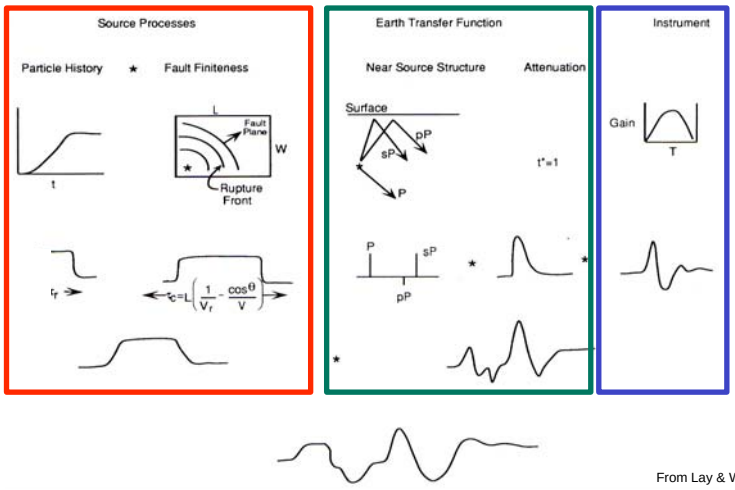

From Lay & Wallace, 1995

Basic equations

Theory of seismic waves & seismic sources

- A few equations of seismic sources and seismic waves based on dynamic elasticity; no derivations ...
  - We need a source representation that captures all possible mechanisms that excite seismic waves.
  - We want to be able to examine the radiated seismic waves at many locations, so far-away from the source (far-field) as well as very close to the fault (near-field).
  - We need to include the potential complexity of the rupture process and the wave propagation through a geologically complicated Earth.

Basic concepts and equations

- We want displacements ***u*** = ***u(x,t)*** as function of space and time in a volume *V* (surface *S*) due to forces applied within and at the surface of that volume.
- We assume small deformations (infinitesimal strain theory) and use tractions ***T*** and stresses $\boldsymbol{\tau}$ to analyze the internal forces acting mutually between adjacent particles in the volume.

- momentum equation $$\frac{\partial}{\partial t}\int\int\int_V \rho\frac{\partial \mathbf{u}}{\partial t}dV = \int\int\int_V \mathbf{f}dV + \int\int_S \mathbf{T}(\mathbf{n})dS$$
- symmetric stress tensor $$T_i = \tau_{ij}n_j$$
- equation of motions $$\rho\ddot{u}_i = f_i + \tau_{ij,j}$$
- stress-strain relation $$\tau_{ij} = c_{ijkl}\epsilon_{kl}$$

$$\tau_{ij} = \lambda\epsilon_{kk}\delta_{ij} + 2\mu\epsilon_{ij}$$

Towards seismic sources

- To parameterize seismic sources we need some theorems that relate the displacement ***u(x,t)*** to initial conditions and forces:
  - **Uniqueness theorem**: The displacement field ***u = u(x,t)*** in the volume *V* with surface *S* is **uniquely** defined after time t_0 by the initial values of displacement and particle velocity in *V*, and by the values of the body forces ***f***, the tractions ***T*** over any part S_1 of *S* for times $t \geq t_0$, and the displacements over the remainder S_2 of *S* ($S_1 + S_2 = S$).
  - **Betti's theorem**: Given a displacement field ***u = u(x,t)*** due to body forces ***f,*** boundary conditions on *S,* and initial conditions at time *t = 0*. Given also a field ***v = v(x,t)*** due to body forces ***g***. These two fields are strictly related through the corresponding tractions, irrespective when the forces act
- We also introduce the **elasto-dynamic Green's function** $\mathbf{G}(\mathbf{x}, t; \xi, \tau)$**:** the i[th] component of the displacement at ***(x,t)*** for a unit impulse in direction *n* at ***(x,t)***.
  - The Green's function obeys spatial and temporal reciprocity

Representation Theorem

- After considerable algebra, the following representation theorem emerges:

$$u_n(\mathbf{x},t) = \int_{-\infty}^{\infty} d\tau \int\int\int_V f_i(\xi,\tau)\cdot G_{in}(\xi,t-\tau;\mathbf{x},0)\,dV + \int_{-\infty}^{\infty} d\tau \int\int_S [G_{in}(\xi,t-\tau;\mathbf{x},0)\cdot T_i(\mathbf{u}(,\xi,\tau),\mathbf{n})]\,dS - \int_{-\infty}^{\infty} d\tau \int\int_S [u_i(\xi,\tau)\cdot c_{ijkl}\cdot n_j\cdot G_{kn,l}(\xi,t-\tau;\mathbf{x},0)]\,dS$$

- The displacement field ***u(x,t)*** is composed of three terms: the contributions from the body forces ***f*** acting in the volume, the contributions due to tractions ***T*** (surface or contact forces) and the contributions from some internal displacement ***u***. Each contribution involves a Green's function term.

- We simplify and rewrite this expression; neglecting body forces & surface tractions, we consider the displacement fields due to internal dislocation sources

Volterra's theorem

- Displacement field due to internal dislocations:

$$u_n(\mathbf{x},t) = \int_{-\infty}^{\infty} d\tau \int\int_\Sigma [u_i(\xi,\tau)]\cdot c_{ijpq}\cdot \nu_j \cdot \frac{\partial}{\partial \xi_q} G_{np}(\mathbf{x},t-\tau;\xi,0)\,d\Sigma$$

- $u_n(\mathbf{x},t)$ — n[th] component of the observed displacement field at ***x***, *t*
- $[u_i(\xi,\tau)]$ — i[th] component of the displacement at the source as a function of position ***x*** on the fault plane and time *t*
- $G_{np}(\mathbf{x},t-\tau;\xi,0)$ — system response in *n*-direction due to unit impulse in direction *p* on the fault plane at ***x***, *t*
- $\frac{\partial}{\partial \xi_q} G_{np}(\mathbf{x},t-\tau;\xi,0)$ — generalized force couple in x_q-direction and force in *p*-direction
- c_{ijpq} ν_j — elasticity tensor; normal to the rupture plane

Seismic Sources

Further simplifications

- Simplifing Volterra's theorem we obtain the following set of equations

$$u_n(\mathbf{x},t) = \int\int_\Sigma [u_i(\xi,\tau)] \cdot c_{ijpq} \cdot \nu_j * \frac{\partial}{\partial \xi_q} G_{np}\, d\Sigma$$

$$m_{pq} \equiv [u_i] \cdot c_{ijpq} \cdot \nu_j$$

$$u_n(\mathbf{x},t) = \int\int_\Sigma m_{pq} * \frac{\partial}{\partial \xi_q} G_{np}\, d\Sigma$$

$$u_n(\mathbf{x},t) = M_{pq} * G_{np,q}$$

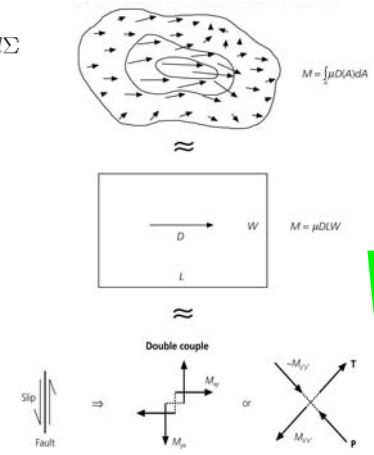

Rupture Complexity → Double-Couple Point Source

Moment Tensor

Characterization of force distribution

- Graphical view of the nine force couples of the seismic moment tensor M_{pq}

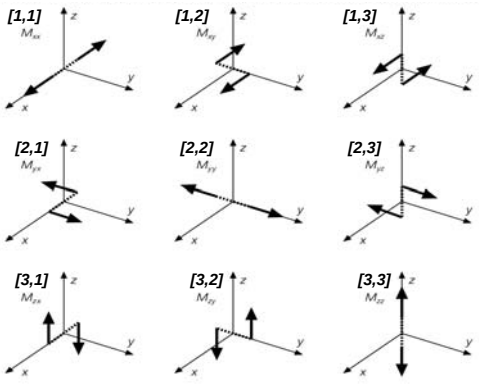

$$\begin{pmatrix} M_{xx} & M_{xy} & M_{xz} \\ M_{yx} & M_{yy} & M_{yz} \\ M_{zx} & M_{zy} & M_{zz} \end{pmatrix}$$

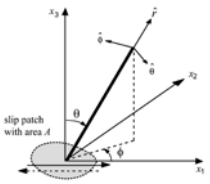

$$log_{10}(M_0) = 1.5 \cdot M_w + \ 9.05$$

$$M_0 = \mu \cdot \overline{D} \cdot A = \mu \cdot [\overline{u}] \cdot A$$

Inverting for the moment tensor

- Using seismic data, we can formulate a linear inverse problem for the six independent moment-tensor component;

$$u_i(t) = \sum_{j=1}^{6} G_{ij}(t) m_j$$

- G_{ij} is a "Green's function" for the i[th] seismometer (including instrument response and Earth structure) due to moment tensor component m_j
- Since we have many seismograms, we write a vector-matrix equation containing seismograms at *n* stations

$$\underline{u} = \underline{\underline{G}}\,\underline{m}$$

- $\underline{\underline{G}}$ is now a Green's function matrix, with as many rows as seismometers, and exactly six columns for the independent moment-tensor components

$$\begin{pmatrix} u_1 \\ u_2 \\ \cdot \\ \cdot \\ \cdot \\ u_n \end{pmatrix} = \begin{pmatrix} G_{11} & G_{12} & G_{13} & G_{14} & G_{15} & G_{16} \\ G_{21} & G_{22} & G_{23} & G_{24} & G_{25} & G_{26} \\ \cdot & \cdot & \cdot & \cdot & \cdot & \cdot \\ \cdot & \cdot & \cdot & \cdot & \cdot & \cdot \\ \cdot & \cdot & \cdot & \cdot & \cdot & \cdot \\ G_{n1} & G_{n2} & G_{n3} & G_{n4} & G_{n5} & G_{n6} \end{pmatrix} \begin{pmatrix} m_1 \\ m_2 \\ m_3 \\ m_4 \\ m_5 \\ m_6 \end{pmatrix}.$$

23

Inverting for the moment tensor

- This linear system of equations is over-determined, as we have more equations (*n*) than unknowns (6); to solve this system in a least-square sense the so-called "*generalized inverse of G*" can be used

$$m^{est} = \left[G^T G\right]^{-1} G^T u$$

- The quality of the solution of the moment tensor components m_j depends on the Green's function
  - If G_{ij} is zero, m_j has no effect on the seismogram
  - Since this inversion for m_j is essentially a division of the seismogram by G_{ij}, small errors or noise in the data produce spuriously large values of m_j
- Formally inverting seismic data for the full moment-tensor is done routinely at a number of monitoring agencies (e.g. CMT, NEIC) using long-period body-waves or preferably surface waves

24

Inverting for the moment tensor

- A selection of moment-tensor solutions of globally recorded earthquakes (http://www.globalcmt.org/)

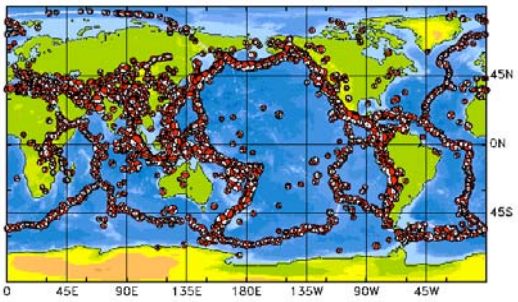

The 2002 M 7.8 Denali EQ

```
110302J CENTRAL ALASKA
Date: 2002/11/ 3 Centroid Time: 22:13:28.0 GMT
Lat= 63.23 Lon=-144.89
Depth= 15.0 Half duration=23.5
Centroid time minus hypocenter time: 47.0
Moment Tensor: Expo=27 0.513 -6.038 5.525 0.183 2.615 -3.937
                       Mrr   Mθθ   Mφφ   Mrθ   Mrφ   Mθφ
Mw = 7.8 mb = 7.0 Ms = 8.5 Scalar Moment = 7.48e+27
Fault plane: strike=296 dip=71 slip=171
Fault plane: strike=29 dip=82 slip=19
```

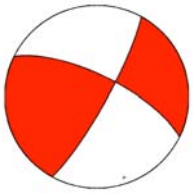

Denali: aftershocks and major sub-sources

- Is the moment-tensor representation useful in this case?

Fig. 2. Locations of principal earthquakes and aftershocks. Stars show the hypocenters of the 23 October M_W 6.7 and 3 November M_W 7.9 earthquakes, with double-difference relocated aftershocks shown in green and orange, respectively. Focal mechanisms show the first motion solution for the M_W 6.7 earthquake and the 3 subevents (sub1 to -3) determined for the M_W 7.9 earthquake. Mapped surface rupture shown as heavy magenta line; red lines indicate other faults. The inset cross section shows schematic faults and $M_L \geq 2.5$ aftershocks in the bracketed zone across the Susitna Glacier (SG) thrust, inferred to splay off the Denali (Den) fault. Cross, mainshock.

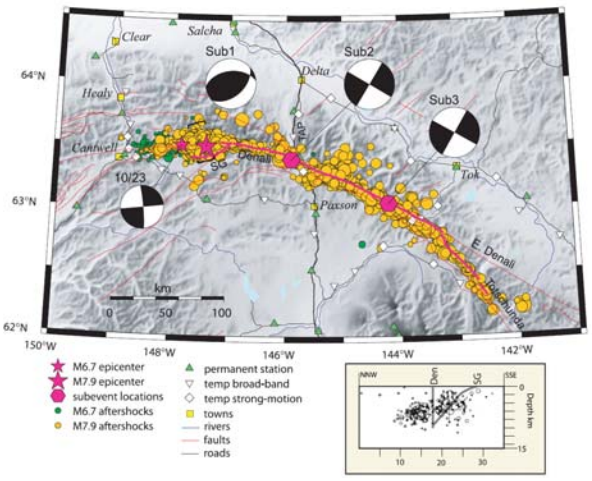

Eberhardt-Phillips et al., Science (2003)

Moment Tensor

Multiple subsources to explain waveforms

- An example: modeling the complex rupture of the M 7.5 1976 Guatemala earthquake

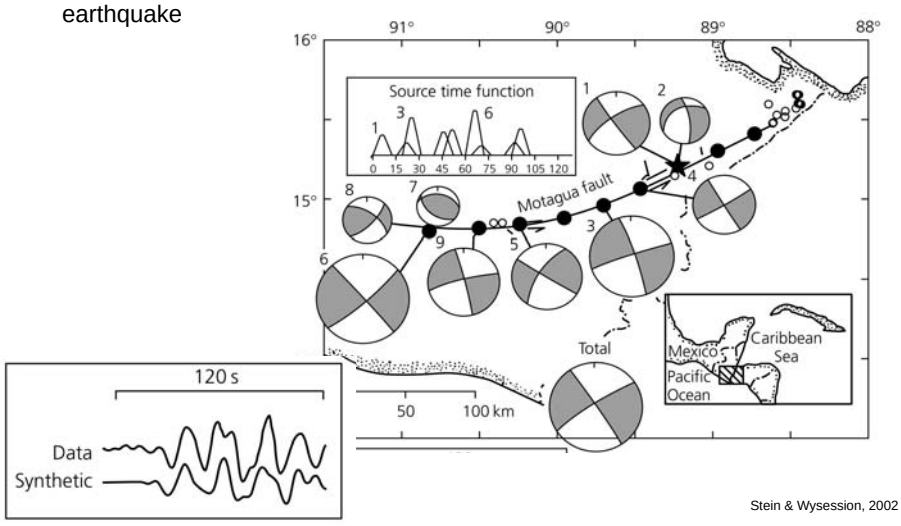

Stein & Wysession, 2002

Finite-Fault Model

Denali: a more comprehensive rupture model

- Based on GPS and seismic data, using 4 fault segments, each divided into many small patches (sub-faults)

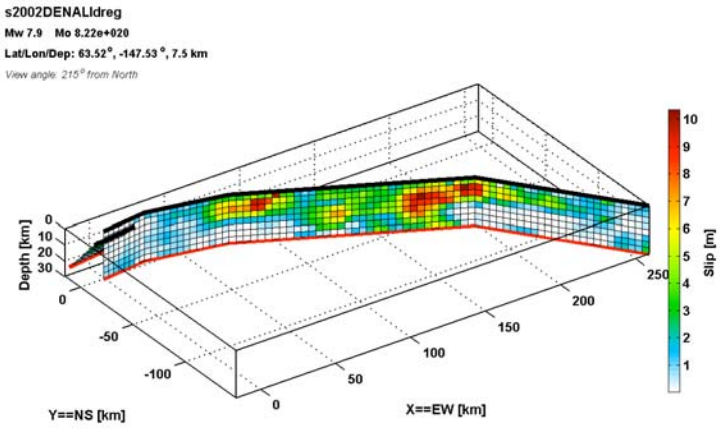

Mai (2007), after results by Oglesby et al, (2004)

We start again at the representation theorem

- **The representation is used** to invert for the slip-time history on the fault plane using seismic observation

$$u_n(\mathbf{x},t) = \int_{-\infty}^{\infty} d\tau \int\int_{\Sigma} [u_i(\xi,\tau)] \cdot \nu_j \cdot c_{ijpq} \cdot \frac{\partial}{\partial \xi_q} G_{np}(\mathbf{x}, t-\tau; \xi, 0) d\Sigma$$

- Assuming we know **Earth structure** reasonably well, we can examine seismic observations in order to learn about the **earthquake source properties**.
- Remember: this representation theorem does not contain any information about the detailed physics (stresses, friction) of the dynamic earthquake rupture process!

The „standard“ (multi-time-window) approach

- Linearized inversion, using the representation theorem, by making the following assumptions (based on Olson & Apsel, 1982; Hartzell & Heaton, 1983)
  - The elementary slip function is simple and identical for all points on the fault
  - The slip-history at each point is represented by summing a number of elementary slip functions, lagged in time (multi-time window)
  - The rise-time is constant
  - The rupture speed is constant

$$\Delta t_{\text{trig}} = \frac{R}{Vr} + \Delta tw \cdot (itm - 1)$$

$$u_n(\mathbf{x},t) = \sum_{itm=1}^{\text{ntm}} \sum_{is=1}^{\text{ns}} \sum_{if=1}^{\text{nf}} m(if,is,itm) \times \int \left[u_{\text{unit}_{is}}(\tau - \Delta t_{\text{trig}}) \right] \times c_{i(is)jkl}(\xi) n_j G_{kn,l}(\mathbf{x}, t-\tau; \xi(if), 0)\, \mathrm{d}\tau$$

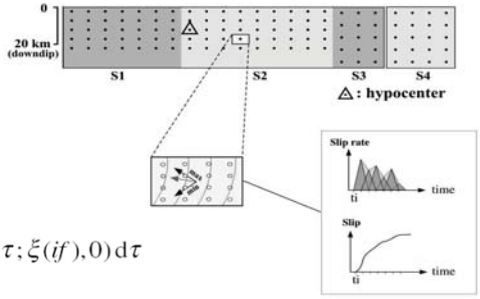

The „standard“ (multi-time-window) approach

- As before, we have a linear system of equations that can be solved by common strategies

$$\underline{d} = \underline{\underline{G}}\,\underline{m} = \sum_j G_{ij} m_j$$

include smoothing

$$\begin{bmatrix} \underline{d} \\ \underline{0} \end{bmatrix} = \begin{bmatrix} \underline{\underline{G}} \\ \lambda \underline{\underline{S}} \end{bmatrix} \underline{m}$$

S represents a smoothing matrix that accounts for variations in the model parameters with distance and time (the farther apart subfaults are, the larger a difference is allowed); λ has to be determined by trial-and-error, or some statistical information criterion.

$$\begin{bmatrix} d_1 \\ d_2 \\ \vdots \\ d_1 \\ d_2 \\ \vdots \\ d_1 \\ d_2 \\ \vdots \end{bmatrix} \cong \begin{bmatrix} G_{11} & G_{12} & \cdots & G_{1m} \\ G_{21} & G_{22} & \cdots & G_{2m} \\ \vdots & \vdots & & \\ G_{11} & G_{12} & \cdots & G_{1m} \\ G_{21} & G_{22} & \cdots & G_{2m} \\ \vdots & \vdots & & \\ G_{11} & G_{12} & \cdots & G_{1m} \\ G_{21} & G_{22} & \cdots & G_{2m} \\ \vdots & \vdots & & \end{bmatrix} \begin{bmatrix} s_1 \\ s_2 \\ \vdots \\ \vdots \\ s_m \end{bmatrix}$$

(time) data points station 1 — (time) data points station 2 — (time) data points station N

Subfault 1 synthetics — Subfault 2 synthetics — Subfault m synthetics

s_1 Dislocation in subfault 1; s_2 Dislocation in subfault 2; s_m Dislocation in subfault m

- **The 1999 Izmit earthquake: a combined inversion**

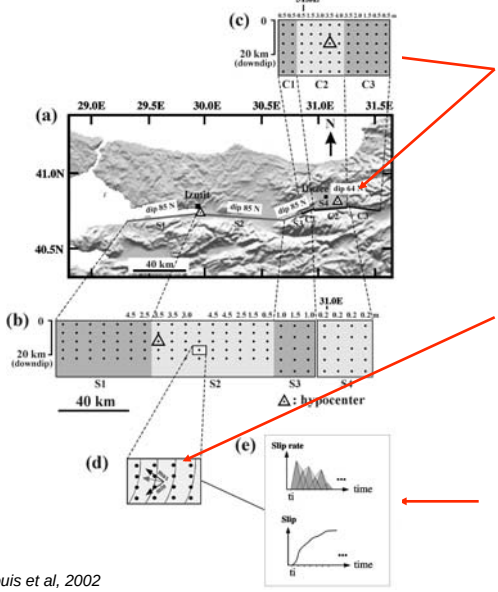

True geometry approximated with several straight segments, each with different dip and strike.
Each segment divided into a number of subfaults; one subfault is taken as the hypo center (triangle here)

FOR NEAR-SOURCE DATA: need to consider effect of rupture propagation within each subfault if the subfaults are large (i.e. > 2x2 km²). If the rake angle is allowed to vary the inversion becomes non-linear. Also the trigger time at which each subfault starts radiating is a free parameters

To account for complicated slip-velocity functions, a sequence of overlapping triangular slip-functions is used whose number and lengths is fixed a priori. The combined slip function (bottom) is given by the envelope of the individual triangular functions, and comprises some of the dynamic complexity expected.

Delouis et al, 2002

Finite-Source Inversion

- **The 1999 Izmit earthquake: a combined inversion**

GPS

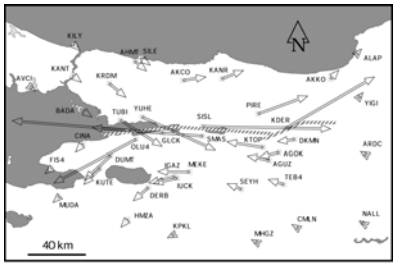

InSAR

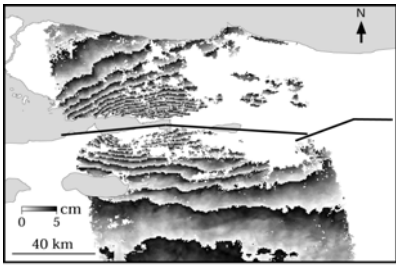

Teleseismic

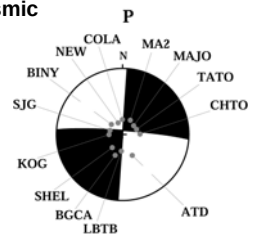

Near-field seismic data

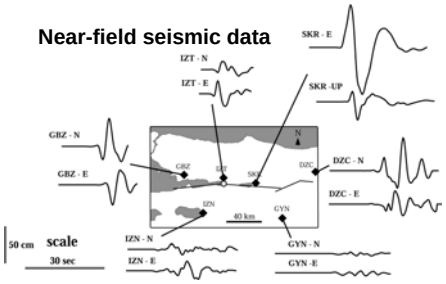

Delouis et al, 2002

Finite-Source Inversion

- **The 1999 Izmit earthquake: a combined inversion**

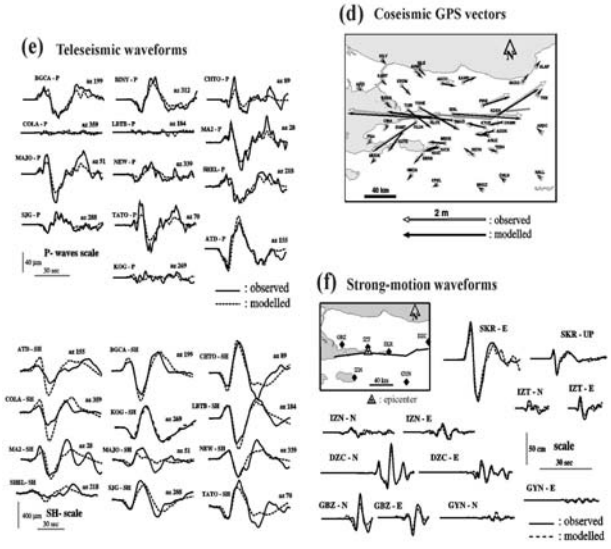

Note the difference between observed and modeled GPS data: such inversions cannot match all the details of the observations, i.e. the small-scale variability is not accounted for (part of the solution space remains inaccessible for the inversion)

Seismic data can only be fit at relatively low frequencies, and still discrepancies remain. High-frequency components are not modeled, which may be due to the source OR the wave-propagation (Earth structure, Green's functions).

Delouis et al, 2002

Finite-Source Inversion

The 1999 Izmit earthquake: a combined inversion

- GPS and InSAR data only constrain the final static slip on the fault.
- GPS and InSAR are very useful to constrain the geometry and the shallow displacement.
- Seismic data also constrain the temporal rupture evolution, but the inversion is ill-posed.

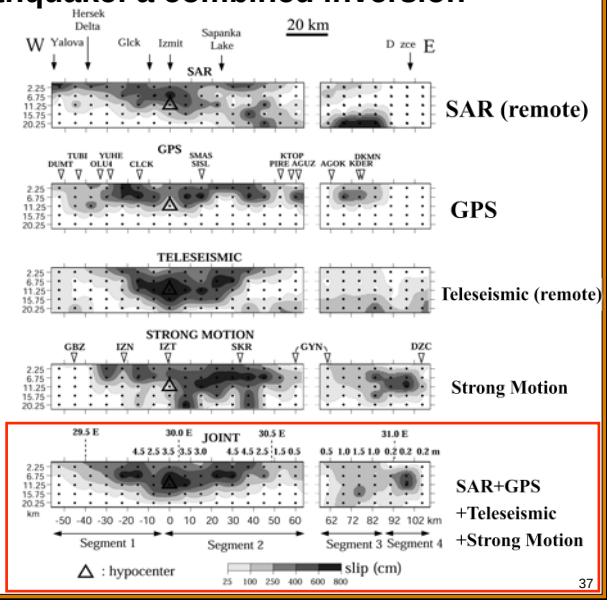

Delouis et al, 2002

37

Finite-Source Inversion

- **Other results for the same earthquake**, obtained by different research teams using different data sets, source parameterizations, and different inversion algorithms

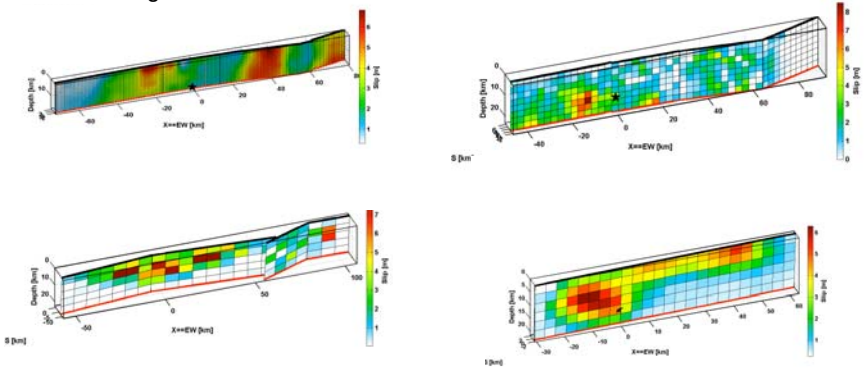

- **Notice large differences between these models, owing to**
  - **different inversion methods, inversion parameterizations**
  - **different data and data processing**
  - **different subjective choices of the modeler**

38

Finite-Source Inversion

Where do the differences between models originate? What are the uncertainties in these source models? How to quantify them?

- Effects of geometric parameterization (source dimensions & discretization)
- Effects of data selection (data type, data distribution, data weighting or combination)
- Effects of the chosen misfit norms (perhaps a combination of different misfit measures is more useful)
- Effects of inversion algorithms & their application (regularization, tuning, modeler choices, ...)

→ **Need to establish "quality standards" for source inversions and specific "standardized tests and agreed-upon procedures" such that the quality of any given model can be assessed.**

39

Recent progress

- **M 6 Parkfield earthquake, very well recorded; velocity structure and fault geometry well known**

Strong-motion sites

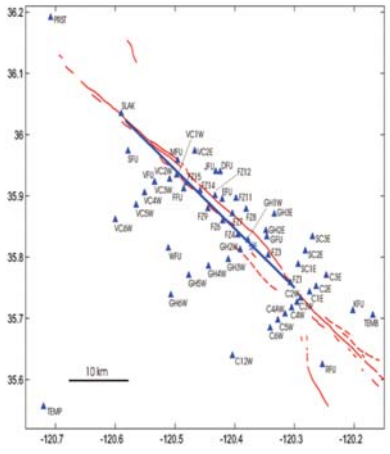

Horizontal static displacements

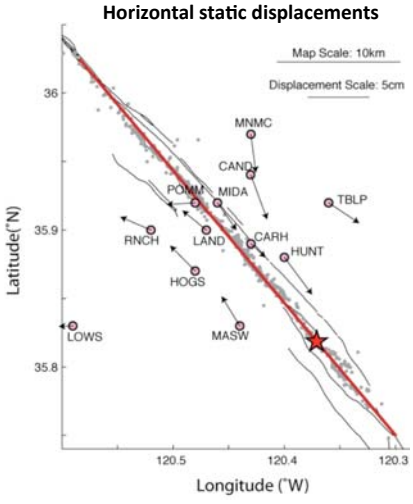

40

Recent progress

- M 6 Parkfield earthquake, very well recorded; velocity structure and fault geometry well known

Hartzell et al, 2007

Linearized, different rupture speed and data corrections

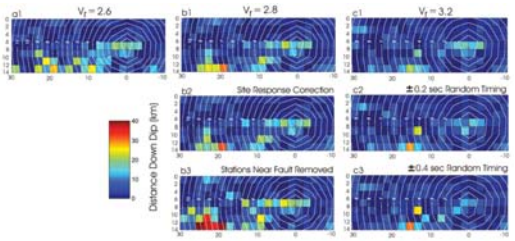

Non-linear, L1 and L2-norm

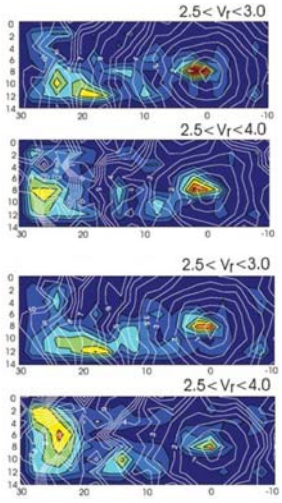

Linearized, different slip function, different data

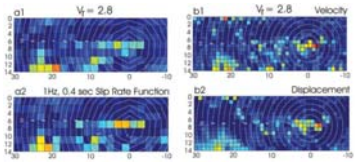

41

Recent progress

- M 6 Parkfield earthquake, very well recorded, velocity structure and fault geometry well known

Liu et al, 2006

Non-linear inversion using strong motion data

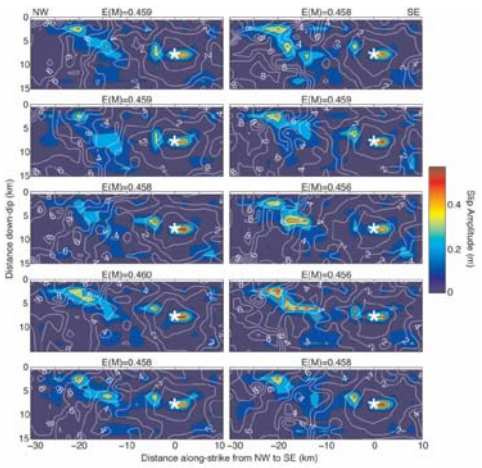

Statistics from these models

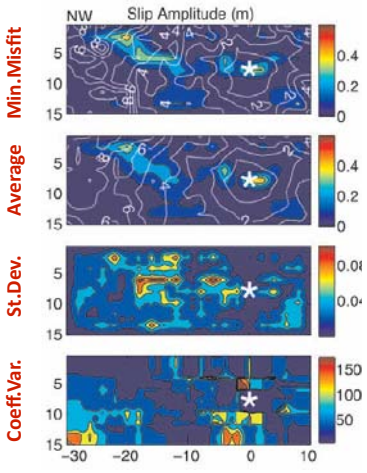

42

Recent progress

- **Bayesian approach to kinematic source inversion**

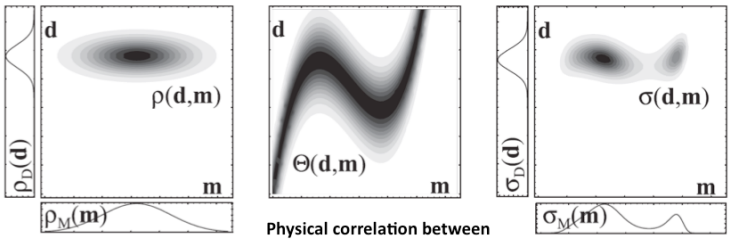

Prior information on model parameters and data

Physical correlation between d and m, as predicted by a nonexact physical theory

Posterior state of information

COMPUTING THE POSTERIOR:

- **Sampling algorithm (e.g. Metropolis; Mosegaard and Tarantola (1995))**
- **Two step procedure: searching + appraising (Sambridge, 1999):**
  1. **Search of the model space**
  2. **From the entire ensemble of models, computation of a geometric approximation of the true posterior by means of a Neighborhood algorithm**

43

Recent progress

- **Synthetic test case**
- **Non-linear optimization using an Evolutionary Algorithm; the model space is sampled generating ~10^6 earthquake models**
- **Based on this large sample size we perform Bayesian estimation to map *the a posteriori distribution* of the model parameters (MCMC sampler)**

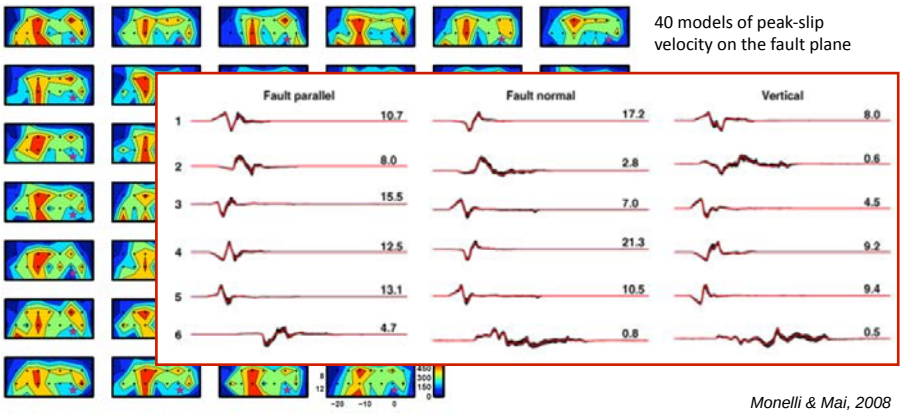

40 models of peak-slip velocity on the fault plane

Monelli & Mai, 2008

44

Recent progress

- Synthetic test case
- Non-linear optimization using an Evolutionary Algorithm; the model space is sampled generating ~10^6 earthquake models
- Based on this large sample size we perform Bayesian estimation to map ***the a posteriori distribution*** of the model parameters (MCMC sampler)

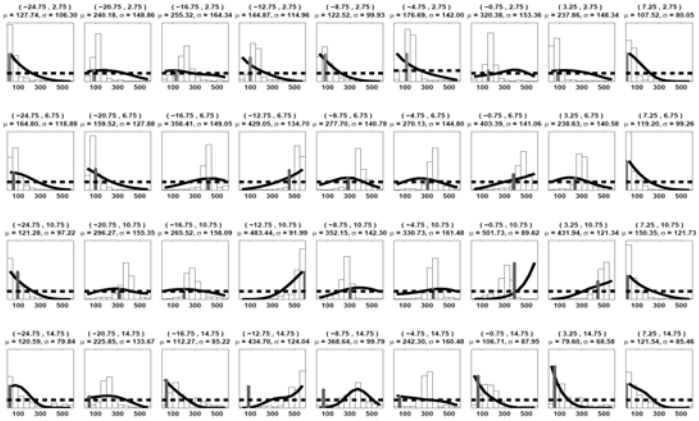

1D-marginals for each node on the fault: --

- - prior

--- posterior

hist: 'raw marginal'

Monelli & Mai, 2008

Recent progress

- **Inversion for the 2000 M 6.8 Tottori earthquake**

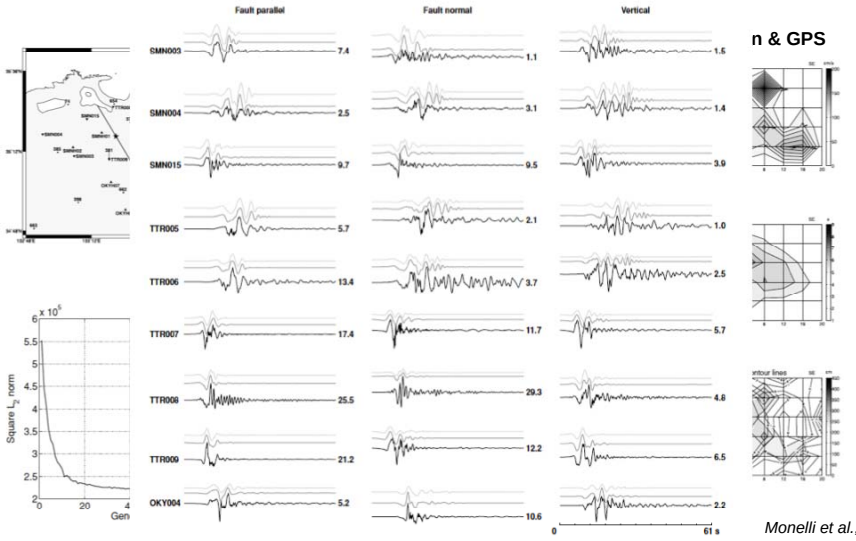

n & GPS

Monelli et al., 2009

Recent progress

- **Inversion for the 2000 M 6.8 Tottori earthquake**

To generate samples according to σ_d^{m-gps}, the sampling algorithm requires solving the forward modelling for the GPS data prediction. With this additional calculation, each random walk, produced 300 000 models in approximately the same computation time (~35 days). From each random walk we extracted 3000 approximately independent samples that we then merged to estimate the corresponding marginals. Even with a smaller number of samples, we observed that each single random walk was able to produce approximately the same marginal, indicating therefore an acceptable convergence.

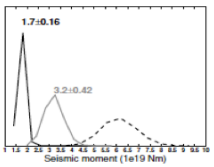

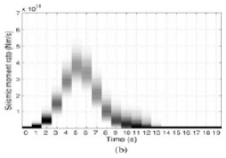

marginals of peak slip-velocity on the fault, after MCMC resampling

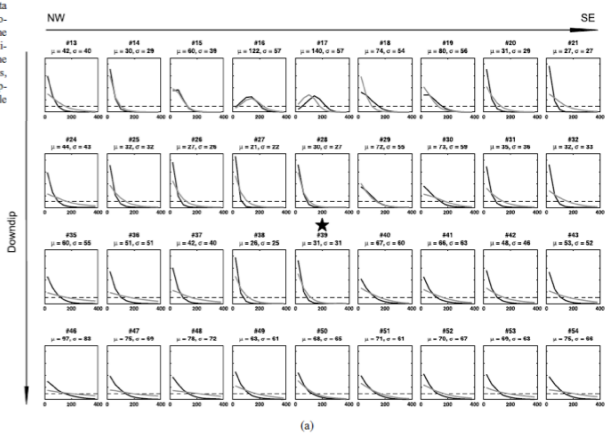

Monelli et al., 2009

47

Verification & Validation

The much needed next steps include verification & validation

- Verification of the forward-modeling codes and inversion techniques
- Validation & benchmarking against synthetic examples with known solutions
- Cooperation between the various source inversion teams to define the “best” source-inversion strategies, in terms of
  - how to parameterize the inversion (depending on data availability)
  - what misfit norm(s) to choose
  - how to quantify the uncertainty in the inverse solution
  - how to disseminate source-inversion results

- **The SPICE blindtest on earthquake source inversion lives on**

48

Verification & Validation

The much needed next steps include verification & validation

- eqsource.webfactional.com/wiki

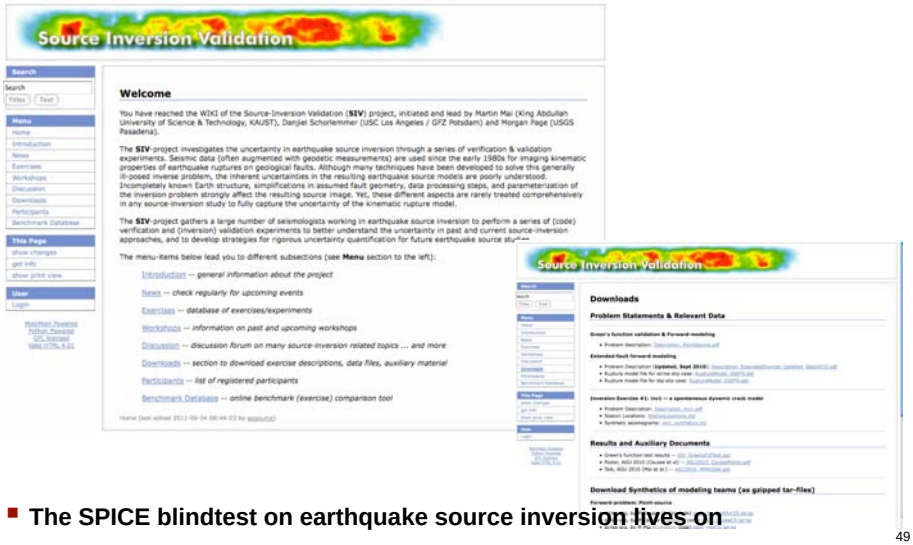

- The SPICE blindtest on earthquake source inversion lives on

QUEST, July 12-17, 2011

Verification & Validation

The much needed next steps include verification & validation

- eqsource.webfactional.com/db/introduction

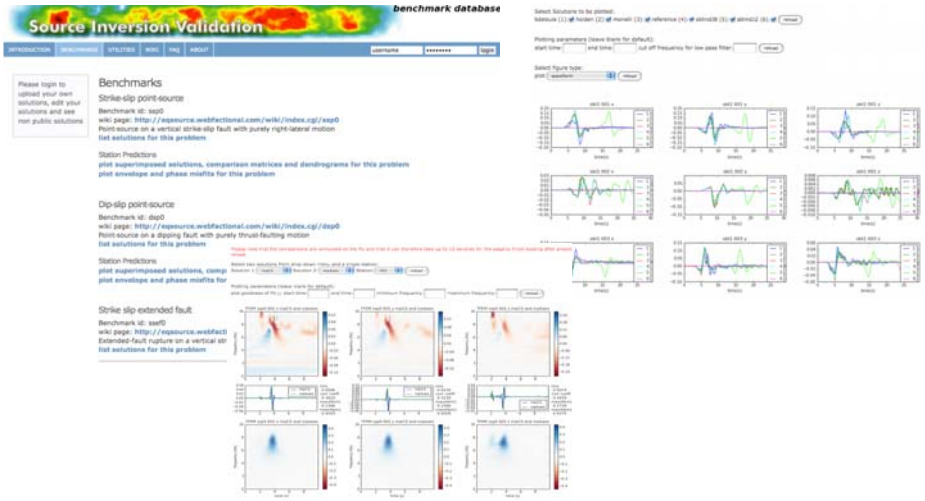

- The SPICE blindtest on earthquake source inversion lives on

Summary

Earthquake source inversion is a hard problem

- Some people considered the problem solved a few years ago!
- We want to be able to rigorously quantify the uncertainties in source inversions, and clearly distinguish the stable robust features from unstable artefacts
- We need clear strategies to tackle the source inversion problem so that it becomes reproducible, including data selection & data processing
- We need innovative ways to include a priori constraints, how to utilize different data sets, and how to include constraints from rupture dynamics into the kinematic source inversion

Additional Slides